Macrocyclic π-Conjugated Carbopolyanions and Polyradicals Based upon Calix[4]arene and Calix[3]arene Rings

Andrzej Rajca,* Suchada Rajca, and Shailesh R. Desai

Contribution from the Department of Chemistry, University of Nebraska, Lincoln, Nebraska 68588-0304

Received August 17, 1994[⊗]

Abstract: Calix[4]arene- and calix[3]arene-based polyether precursors to polyradicals are synthesized. π-Conjugated carbanions, such as calix[4]arene-based tetraanion and calix[3]arene-based trianion, are prepared and studied using NMR spectroscopy and voltammetry. A 4-fold-symmetric conformer for the tetraanion and two non-interconverting conformers (3-fold- and 2-fold-symmetric) for the trianion are found on the NMR time scale. Oxidation of the tetraanion gives the corresponding calix[4]arene-based $S = 2$ tetraradical. However, ESR spectroscopy suggests that the predominant product from oxidation of calix[3]arene-based trianion is the corresponding triradical dimer. The related calix[3]arene-based $S = 1$ diradical is found to be monomeric. Additional characterization of octaradical $\mathbf{1}^{8\bullet}$ and pentaradical $\mathbf{2}^{5\bullet}$, which were described in a preliminary communication, is presented.

Introduction

Synthesis of very-high-spin mesoscopic-size molecules is a challenging and important problem related to the recent topic of organic magnetism.[1,2] In order to obtain very-high-spin molecules, strong intramolecular ferromagnetic coupling between "unpaired" electrons must be maintained. The necessity for the multisite interaction creates formidable synthetic difficulties such as the following: (1) the yield for site generation (p) has to be ultra-high for even a modest yield of molecules with all sites intact, e.g., the yields of intact molecules with 4, 8, and 90 sites for $p = 0.95$ (95% yield per site) would be 81%, 66%, and 1%; (2) defects, which we define as failures to generate an interacting site, may pose an obstacle to an effective interaction between the remaining sites.[3,4] The second problem is especially relevant to strongly spin coupled polyradicals, where the sites (with "unpaired" electrons) are formally incorporated in the coupling paths connecting the sites.[1e,5] In the examples below, the sites, paths, and defects are represented with dots, bars, and open circles, respectively.

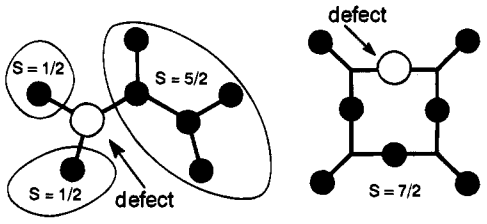

A defect at an inner site affects the spin coupling, depending on the connectivity between the sites: (i) spin coupling is interrupted by dividing a *linear* or *dendritic* polyradical into uncoupled parts with lower spin, (ii) spin coupling is preserved in a *macrocyclic* polyradical with ≤ 1 defect.[6] Polyradicals in (i) and (ii) are labeled as 0-proof and 1-proof, respectively.[1e]

In the preliminary communication, macrocyclic octaradical $\mathbf{1}^{8\bullet}$ and its acyclic pentaradical analogue $\mathbf{2}^{5\bullet}$ were reported. Magnetization measurements for $\mathbf{1}^{8\bullet}$ indicated $S = 4$ ground state and negligible interruption of spin coupling by defects.[6]

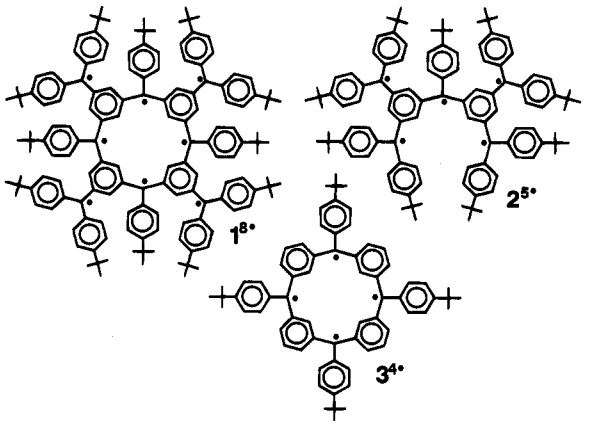

The goal of of the present work is to determine the spin coupling in the calix[n]arene-based ($n = 3$, 4) polyradicals. In addition to further characterization of $\mathbf{1}^{8\bullet}$ and $\mathbf{2}^{5\bullet}$, the parent calix[4]arene-based π-conjugated system, tetraradical $\mathbf{3}^{4\bullet}$, the related calix[3]arene-based diradical **4-H**$^{2\bullet}$, and the dimer of triradical $\mathbf{4}^{3\bullet}$ are reported. The calix[3]arene-based polyradicals are fragments of the Mataga polymer, which was proposed in 1968;[7] this remarkable π-conjugated two-dimensional honeycomb lattice is 5-proof.[1e]

[⊗] Abstract published in *Advance ACS Abstracts,* January 1, 1995.

(1) Recent reviews on spin-coupled organic molecules: (a) Dougherty, D. A. *Acc. Chem. Res.* **1991**, *24*, 88, (b) Iwamura, H.; Koga, N. *Acc. Chem. Res.* **1993**, *26*, 346, (c) Iwamura, H. *Adv. Phys. Org. Chem.* **1990**, *26*, 179, (d) Borden, W. T.; Iwamura, H.; Berson, J. A. *Acc. Chem. Res.* **1994**, *27*, 109, (e) Rajca, A. *Chem. Rev.* **1994**, *94*, 871.

(2) Reviews on mesocopic-size molecules: Diederich, F. *Nature* **1994**, *369*, 199. Mekelburger, H.-B.; Jaworek, W.; Vogtle, F. *Angew. Chem., Int. Ed. Engl.* **1992**, *31*, 1571. Newkome, G. R., Ed. *Advances in Dendritic Macromolecules*; JAI Press: Greenwich, 1994; Vol. I.

(3) Rajca, A.; Utamapanya, S. *J. Am. Chem. Soc.* **1993**, *115*, 10688.

(4) Iwamura's nonacarbene is an example of a high-spin molecule with very high p: Nakamura, N.; Inoue, K.; Iwamura, H. *Angew. Chem., Int. Ed. Engl.* **1993**, *32*, 872.

(5) Attaching spin sites to a chain (spin-coupling path) as pendants gives only weak coupling so far; a defect at the inner site is expected to further weaken the coupling: Nishide, H.; Kaneko, T.; Igarashi, M.; Tsuchida, E.; Yoshioka, N.; Lahti, P. M. *Macromolecules* **1994**, *27*, 3082. Sasaki, S.; Iwamura, H. *Chem. Lett.* **1992**, 1759.

(6) Rajca, A.; Rajca, S.; Padmakumar, R. *Angew. Chem., Int. Ed. Engl.* **1994**, *33*, 2091.

(7) Mataga, N. *Theor. Chim. Acta* **1968**, *10*, 372.

0002-7863/95/1517-0806$09.00/0

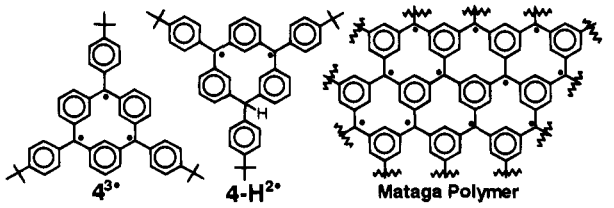

Results and Discussion

A. Synthesis of Polyethers. Synthesis of the tetraether **3-(OMe)$_4$**, triether **4-(OMe)$_3$**, and diether **4-H-(OMe)$_2$**, which are precursors to tetra-, tri-, and diradicals **3⁴•**, **4³•**, and **4-H²•**, is outlined in Figure 1. The macrocyclic rings are constructed by condensation of the bis(aryllithiums), which are generated in situ from **5-OMe** or **5-H** by Br/Li exchange, with diketones such as **6** or 1,3-phenylenebis(4-*tert*-butylphenyl)methanone;[8] the resultant macrocyclic diols are isolated in 30−50% yields.[9] Two isomers, *cis* and *trans* ether−diol, are isolated in the case of calix[3]arene rings; etherification proceeds with retention of configuration giving the corresponding *cis* and *trans* triethers **4-(OMe)$_3$**. Calix[4]arene-based diether−diol and tetraether are isolated as isomeric mixtures.

Synthesis of the polyether precursors to octaradical **1⁸•** and pentaradical **2⁵•**, which follows the methodology analogous to that in Figure 1, is described in the supplementary material.[6] Notably, for more sterically hindered calix[4]arene derivatives, such as hexaether−diol **1-(OMe)$_6$(OH)$_2$** and octaether **1-(OMe)$_8$**, one 2-fold-symmetric isomer has been isolated.[6]

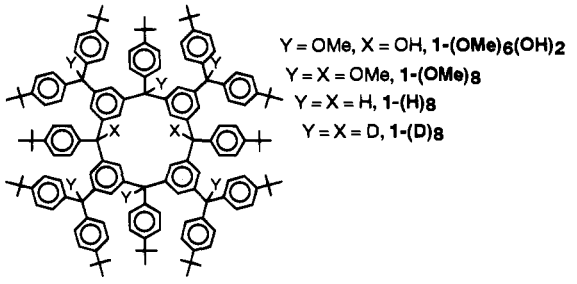

Structural assignments are supported by elemental analyses, FABMS, and NMR spectroscopy. In particular, NMR spectra are consistent with the 3- and 2-fold-symmetric structures for *cis* and *trans* triethers, respectively.

B. Generation of Carbopolyanions and Polyradicals; Quenching Studies.[10,11] Treatment of polyethers **3-(OMe)$_4$**, **4-(OMe)$_3$**, and **4-H-(OMe)$_2$** with an excess of Na/K alloy in tetrahydrofuran (THF) or tetrahydrofuran-d_8 (THF-d_8) for 2−7 days gives solutions of carbanions **3⁴⁻,4M⁺** (M = Na, K), **4³⁻,3M⁺** (M = Na, K), and **4-H²⁻,2M⁺** (M = Na, K), respectively (Scheme 1). (Replacement of Na/K alloy with Li metal gives an acceptable yield of tetraanion **3⁴⁻,4Li⁺**, but it fails to produce trianion **4³⁻,3Li⁺**.) The tetra-, tri-, and dianions are oxidized in THF at 180 K with 2+, 1.5+, and 1+ equiv of I_2 to give tetraradical **3⁴•**, the dimer of triradical **4³•**, and diradical **4-H²•**, respectively (Scheme 1). Octaradical **1⁸•** and pentaradical **2⁵•** are obtained by analogous procedures; however, Li metal fails to generate the intermediate octaanion **1⁸⁻**.

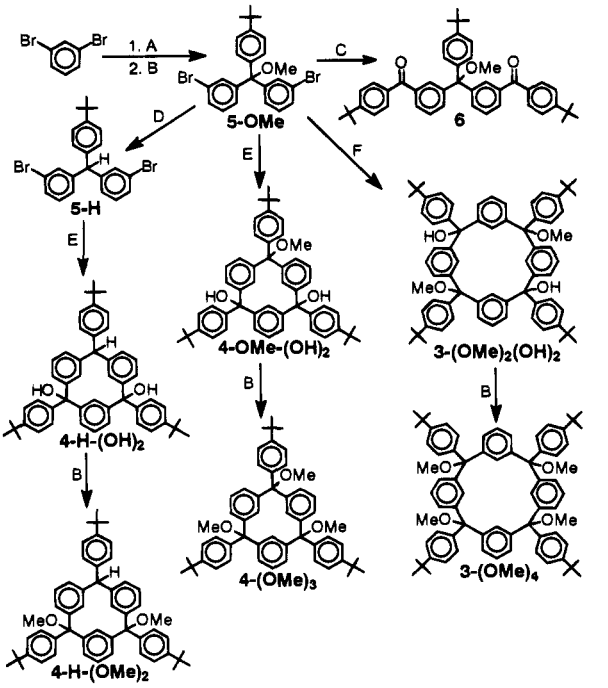

Figure 1. Synthesis of polyethers: A, *n*-BuLi, ether, <0 °C, then 3-bromo-4′-*tert*-butylbenzophenone; B, NaH/THF, MeI; C, (1) *t*-BuLi/THF, −78 °C, (2) 1-(4-*tert*-butylbenzoyl)pyrrolidine; D, $NaBH_4$/TFA/dichloromethane; E, (1) *t*-BuLi/THF, −78 °C, (2) 1,3-phenylenebis(4-*tert*-butylphenyl)methanone; F, (1) *t*-BuLi/THF, −78 °C, (2) diketone **6**.

Scheme 1

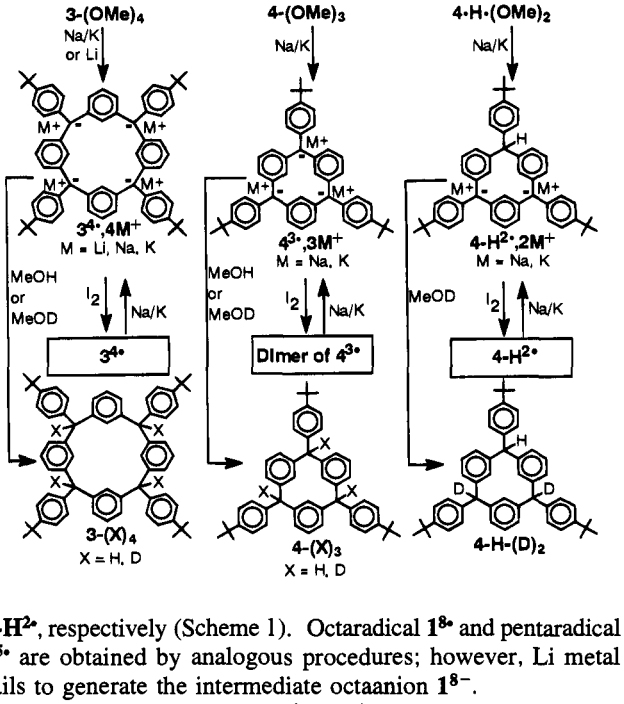

Quenching of tetraanion **3⁴⁻,4M⁺** (M = Na, K, Li) and trianion **4³⁻,3M⁺** (M = Na, K), which are directly generated from the corresponding polyethers, gives the expected products **3-(X)$_4$** and **4-(X)$_3$** (X = H, D) in good yield and 90+% per triarylmethyl site deuterium incorporation (NMR, FABMS).

Quenching studies of polyradicals involve the following procedures. First, a ~10^{-2} M polyradical in THF is diluted (~10-fold) with 2-methyltetrahydrofuran (2-MeTHF). A small portion of this solution is transferred to an ESR tube; the ESR tube is flame-sealed and removed from the reaction vessel (for

(8) 1,3-Phenylenebis(4-*tert*-butylphenyl)methanone: Chaudhuri, J.; Adams, R. F.; Szwarc, M. *J. Am. Chem. Soc.* **1971**, *93*, 5617.

(9) For a related methodology, using dialdehydes, see: Rajca, A.; Padmakumar, R.; Smithhisler, D. J.; Desai, R. S.; Ross, C. R.; Stezowski, J. J. *J. Org. Chem.*, in press.

(10) Acyclic 1,3-Connected Polyarylmethyl Polyanions: Rajca, A. *J. Am. Chem. Soc.* **1990**, *112*, 5889. Utamapanya, S.; Rajca, A. *J. Am. Chem. Soc.* **1991**, *113*, 9242.

(11) Acyclic 1,3-Connected Polyarylmethyl Polyradicals ($S \geq 2$): Rajca, A. *J. Am. Chem. Soc.* **1990**, *112*, 5890. Rajca, A.; Utamapanya, S.; Thayumanavan, S. *J. Am. Chem. Soc.* **1992**, *114*, 1884. Rajca, A.; Utamapanya, S. *J. Am. Chem. Soc.* **1993**, *115*, 2396. Rajca, A.; Utamapanya, S. *Liq. Cryst. Mol. Cryst.* **1993**, *232*, 305.

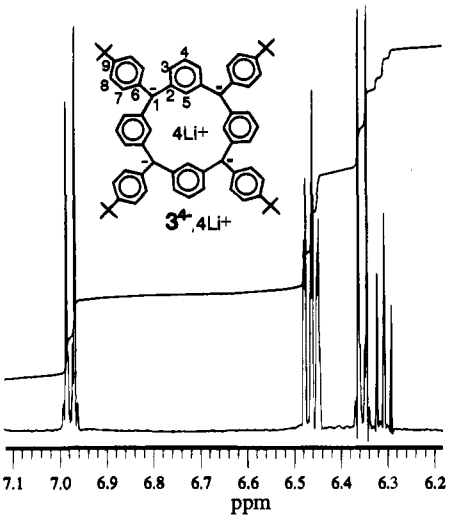

Figure 2. Aromatic region of the ^{1}H NMR (500 MHz) spectrum for tetraanion $\mathbf{3}^{4-}$,$\mathbf{4Li}^+$ in THF-d_8 at 250 K. Expotential and Gaussian multiplications with exponents of −1.3 and +0.7 Hz prior to Fourier transform are used.

ESR spectra, see the following sections). The remaining reaction mixture in the vessel is treated with an excess of Na/K alloy at low temperature and, then, the resultant red solution is quenched with either MeOH or MeOD to give products **3-(X)$_4$**, **4-(X)$_3$**, and **4-H-(X)$_2$** (X = H, D) in good yield and 90+% per triarylmethyl site deuterium incorporation (Scheme 1).

Both *cis* and *trans* isomers of hydrocarbon **4-(H)$_3$** are isolated, starting from *trans* triether **4-(OMe)$_3$**; NMR spectral analysis supports the 3-fold- and 2-fold-symmetric structures, respectively.

From tetraether **3-(OMe)$_4$**, four isomers of hydrocarbon **3-(H)$_4$** are possible and at least three isomers are formed in significant amounts; one 2-fold-symmetric isomer (the fraction with smaller R_f) is isolated from two TLC fractions. The last isomer possesses the NMR spectral pattern analogous to that of the previously isolated 2-fold-symmetric isomers of hexaether−diol **1-(OMe)$_6$(OH)$_2$** and octaether **1-(OMe)$_8$**—precursors to octaradical $\mathbf{1}^{8\bullet}$; that is, the 2-fold symmetry element contains two diagonal triarylmethyl carbons of the calix[4]arene ring. For example, three inequivalent 4-*tert*-butylbenzyl moieties (1/1/2) and two types of inner benzene rings (2/2) are identified in this 2-fold-symmetric isomer of **3-(H)$_4$**.

Quenching of octaanion $\mathbf{1}^{8-}$,$\mathbf{8Na(K)}^+$, derived from $\mathbf{1}^{8\bullet}$, also gives isomeric mixtures (at least three isomers), with a solvent-dependent isomeric content. When ether and 2-MeTHF/THF are used as solvents, a 4-fold-symmetric isomer of **1-(H)$_8$** (high-R_f TLC spot), which is one of the major components, is obtained in pure form; its ^{1}H NMR spectrum shows three types (4/4/4) of 4-*tert*-butylphenyls, two types (4/4) of triarylmethyl protons, and one type (4) of inner benzene ring.

C. NMR Spectroscopy and Voltammetric Studies of Carbotetraanion and Carbotrianion. Variable-temperature NMR spectra for carbanions are obtained in THF-d_8. Electrochemical studies are carried out in THF with tetrabutylammonium perchlorate (TBAP) as supporting electrolyte at 200 K.[10]

Simple ^{13}C NMR spectra of tetraanion $\mathbf{3}^{4-}$,$\mathbf{4Li}^+$ are found both at ambient temperature and at 210 K; i.e., assignments are as follows: aromatic region with 8 lines at 151−115 ppm, triarylmethyl carbons (anionic) with 1 line at 83−84 ppm, *t*-Bu groups with 1 line at ~34 ppm (quaternary) and 1 line at ~32 ppm (Me). ^{1}H NMR spectra consist of two spin systems for the aromatic region and a singlet for the *t*-Bu group (Figure 2); at low temperatures, from 210 to 178 K, the H-3 and H-7 (or H-8) resonances progressively broaden. Probable explanations for the broadening include slow rotation of the 4-*tert*-butylphenyl and/or slow exchange between calix[4]arene conformers on the NMR time scale. ^{6}Li and ^{7}Li NMR spectra at 178 K show a narrow singlet. Therefore, the ^{1}H and ^{13}C NMR data suggest a highly symmetric (C_4 or higher symmetry) structure on the NMR time scale at ambient temperature.

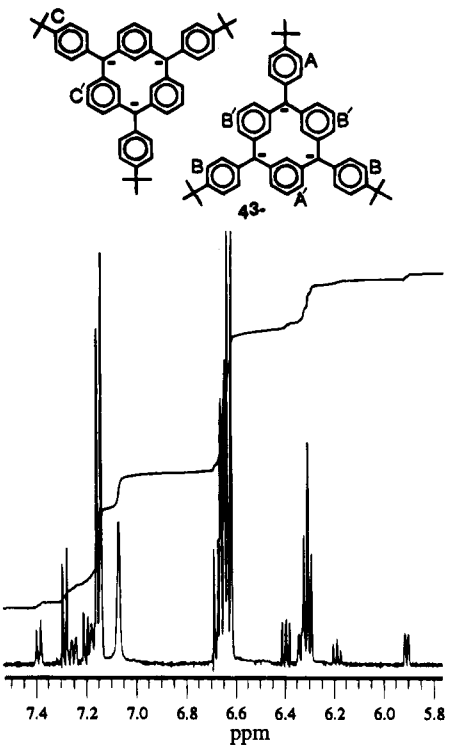

Figure 3. Aromatic region of the ^{1}H NMR (500 MHz) spectrum for trianion $\mathbf{4}^{3-}$,$\mathbf{3Na(K)}^+$ in THF-d_8 at 295 K. Expotential and Gaussian multiplications with exponents of −1.7 and +1.0 Hz prior to Fourier transform are used. The major isomer (3-fold symmetric) has its resonances labeled C and C′*n* (*n* = 1, 2, 3) for the outer and inner benzene rings, where "*n*" refers to the spin multiplicity for vicinal coupling (J = 7−8 Hz). Analogously, the labels for the minor isomer (2-fold symmetric) are A, B and A′*n*, B′*n*. The assignments are given in the Experimental Section.

For the dilute solution of trianion $\mathbf{4}^{3-}$,$\mathbf{3Na(K)}^+$, three spin systems for the inner rings (1/2/10) and three spin systems for the outer rings (1/2/10) may be identified in the aromatic region of the ^{1}H NMR spectrum (Figure 3); ^{1}H−^{1}H COSY correlation confirms the assignment. The 1/2/10 integration ratio is also found for the three singlets in the 1.3−1.1 range, which corresponds to the *t*-Bu groups. These integration ratios change from 1/2/10 to aproximately 1/2/4 in a more concentrated solution. Similar behavior is found in the ^{13}C NMR spectra, which is further confirmed by ^{1}H−^{13}C COSY correlation for nonquaternary aromatic carbons.

NMR spectra for trianion $\mathbf{4}^{3-}$,$\mathbf{3Na(K)}^+$ are best analyzed by assuming the presence of two isomers *cis* and *trans*, which are 3-fold and 2-fold symmetric, respectively, on the NMR time scale, analogous to the corresponding triethers 4-(OMe)$_3$ and hydrocarbons 4-(H)$_3$. The *cis*/*trans* ratio is 3.3/1 and 1.3/1 for the two samples, which are mentioned in the preceding paragraph.

At low temperatures (250−180 K), ^{1}H resonances for rings (A) and (A′) remain sharp even at 210 K; other resonances progressively broaden between 250 and 210 K. At 180 K, a complex spectrum with a large number of broadened resonances is obtained. Therefore, the lowest energy conformations for

calix[3]arene-based trianions may possess very few, if any, elements of symmetry. ^{13}C chemical shifts, which may be related to the negative charges at sp^2-hybridized carbons,[12] follow the patterns found in tetraanion $\mathbf{3}^{4-}$,$\mathbf{4Li}^+$; the extent of delocalization of negative charge to the benzene rings is comparable or slightly greater in trianion $\mathbf{4}^{3-}$,$\mathbf{3Na(K)}^+$ than in tetraanion $\mathbf{3}^{4-}$,$\mathbf{4Li}^+$. For example, ^{13}C chemical shifts for triarylmethyl (anionic) carbons are in the 87−90 and 83−84 ppm ranges for $\mathbf{4}^{3-}$,$\mathbf{3Na(K)}^+$ and $\mathbf{3}^{4-}$,$\mathbf{4Li}^+$, respectively. These similarities extend to previously studied star-branched polyanions.[10] Consequently, the factors influencing charge distribution in their π-conjugated systems, such as out-of-plane distortions, must be comparable for star-branched and macrocyclic 1,3-connected polyarylmethyl polyanions, possibly, with greater degree of planarity for trianion $\mathbf{4}^{3-}$.

Cyclic voltammetry of tetraanion $\mathbf{3}^{4-}$,$\mathbf{4Li}^+$/TBAP at 200 K reveals three reversible oxidation waves (with relative peak currents, i_p, 1:1:2) at $E_p = -1.83$, -1.66, and -1.22 V, respectively, versus SCE. The wave with the largest i_p ($E_p = -1.22$ V) has a symmetrical shoulder, which suggest two waves with similar potentials. Thus, the voltammogram is consistent with the four 1-electron oxidations of the tetraanion to the tetraradical.

Appearance of a cyclic voltammogram for trianion $\mathbf{4}^{3-}$,$\mathbf{3Na(K)}^+$/TBAP at 200 K depends on the scan rate (SR). At SR ≤ 10 mV/s, three reversible oxidation waves with identical i_p are found at $E_p = -1.88$, -1.55, and -1.28 V versus SCE, which may correspond to three 1-electron oxidations of the trianion to the triradical. At SR ≥ 20 mV/s, additional waves with smaller i_p may be discerned at the intermediate values of E_p. A plausible interpretation is that the isomerization or other chemical transformation (e.g., dimerization) of the redox species at (or close to) the Pt-electrode surface is slow on the voltammetry time scale for SR ≥ 20 mV/s; the isomerization might have its analogy in the dynamic behavior of $\mathbf{4}^{3-}$,$\mathbf{3Na(K)}^+$ in solution on the NMR time scale.

D. ESR Spectroscopy and Magnetization Studies of Polyradicals. As expounded in the earlier work, because 1,3-connected polyarylmethyl polyanions and polyradicals differ in the population of nonbonding MO's only, their bonding characteristics, including charge/spin distribution, should be similar.[10,11] Consequently, it is anticipated that the present macrocyclic polyradicals will possess high-spin ground states with substantial energy gaps between the ground states and low-spin excited states.

The results for polyradicals are presented and discussed, in the order related to their structural characteristics, as follows: tetraradical $\mathbf{3}^{4\bullet}$ (calix[4]arene ring), pentaradical $\mathbf{2}^{5\bullet}$ (hyperbranching), octaradical $\mathbf{1}^{8\bullet}$ (calix[4]arene ring and hyperbranching), diradical $\mathbf{4\text{-}H}^{2\bullet}$ (calix[3]arene ring), and dimer of triradical $\mathbf{4}^{3\bullet}$.

(a) **Tetraradical $\mathbf{3}^{4\bullet}$.** The $\Delta m_s = 1$ region of the X-band ESR spectrum for tetraradical $\mathbf{3}^{4\bullet}$ in 2-MeTHF/THF glass at $T = 30$ K is adequately reproduced by computer simulation for an $S = 2$ state (Figure 4). The zero-field splitting (zfs) parameters are $|D/hc| = 0.0033$ cm^{-1} and $|E/hc| = 0$ cm^{-1}.[13,14] The zfs parameters for the present macrocyclic 8-benzene rings

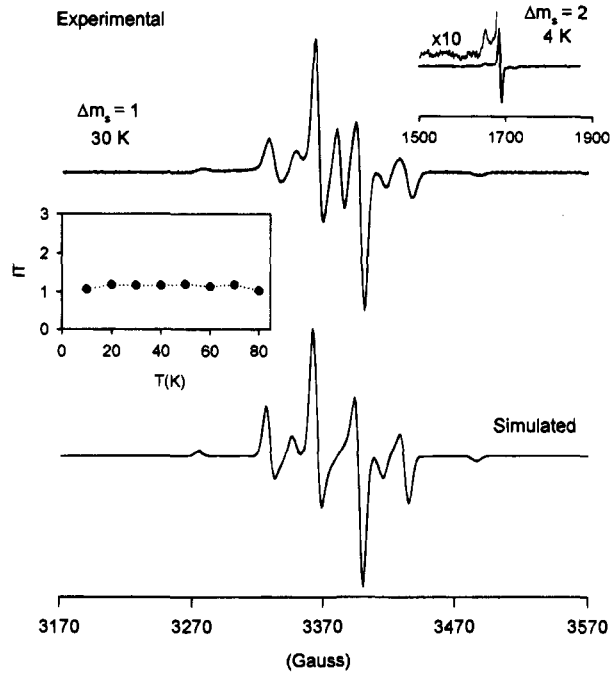

Figure 4. ESR spectroscopy of tetraradical $\mathbf{3}^{4\bullet}$, which was obtained from $\mathbf{3\text{-}(OMe)_4}$ using the Na/K alloy method. Experimental: $\Delta m_s = 1$ and 2 regions of the experimental spectrum in THF/2-MeTHF glass at 30 and 4 K, respectively; plot of the product (IT) of the intensity (I) for the $\Delta m_s = 2$ signal and the temperature (T) versus T. Simulated: simulation of the $\Delta m_s = 1$ region using second-order perturbation theory solution to the spin-only dipolar Hamiltonian for the $S = 2$ state with a Gaussian line width of 6 G and the following zfs parameters: $|D/hc| = 0.0033$ cm^{-1} and $|E/hc| = 0$ cm^{-1}.

tetraradical are only slightly greater than those for the related star-branched 9-benzene rings tetraradical with $|D/hc| = 0.0030$ cm^{-1} and $|E/hc| \approx 0$ cm^{-1}.[11] Probably, the center peak belongs to half-integral spin ($S = {}^1/_2$, ${}^3/_2$) impurity. Because the height of this peak for $S = {}^1/_2$ or $S = {}^3/_2$ should be an order of magnitude more than the highest peak for $S = 2$, the content of these impurities is roughly <10%. (The height of this peak is about twice that for samples of the tetraradical, which are obtained via tetraanions generated from tetraether with Li compared to Na/K alloy.) The $\Delta m_s = 2$ region consists of an intense center line, which is accompanied by weak side peaks, as expected for $S = 2$ (and higher integral spin values).[11] The $\Delta m_s = 3$ transition is not detected; its peak height is anticipated to be an order of magnitude less than that for comparable polyradicals with half-integral spin values such as $S = {}^3/_2$ and ${}^5/_2$, for which it may be observed (*vide infra*).[11]

The ESR spectra in the both $\Delta m_s = 1$ and 2 regions at 4 K (with some loss of intensity due to microwave saturation) are very intense. The plot of the product (IT) of the intensity (I) for the center line of the $\Delta m_s = 2$ signal and the temperature (T) versus T is constant in the 10−80 K range (Figure 4); similarly, the Curie plot (I vs $1/T$) is linear in this temperature range. Thus, the change in the thermal population of the low-spin excited states is negligible in this temperature range.

The ESR spectroscopy for $\mathbf{3}^{4\bullet}$ strongly supports the $S = 2$ ground state, which is separated from the lowest-lying low-spin excited state by an energy gap (ΔE) greater than thermal energy (RT) in the studied temperature range ($\Delta E \gg RT$). However, near degeneracy of the $S = 2$, 1, 0 states ($\Delta E \ll RT$)

(12) Spiesecke, H.; Schneider, W. G. *Tetrahedron Lett.* **1961**, 468. Rajca, A.; Tolbert, L. M. *J. Am. Chem. Soc.* **1988**, *110*, 871.

(13) For other strongly-coupled $S = 2$ ground state organic tetraradicals, see: Seeger, D. E.; Berson, J. A. *J. Am. Chem. Soc.* **1983**, *105*, 5144, 5146. Seeger, D. E.; Lahti, P. M.; Rossi, A. R.; Berson, J. A. *J. Am. Chem. Soc.* **1986**, *108*, 1251. Novak, J. A.; Jain, R.; Dougherty, D. A. *J. Am. Chem. Soc.* **1989**, *111*, 7618. Jacobs, J. S.; Shultz, D. A.; Jain, R.; Novak, J.; Dougherty, D. A. *J. Am. Chem. Soc.* **1993**, *115*, 1744. Silverman, S. K.; Dougherty, D. A. *J. Phys. Chem.* **1993**, *97*, 13273. Jacobs, J. S.; Dougherty, D. A. *Angew. Chem., Int. Ed. Engl.* **1994**, *33*, 1104.

(14) Simulation of ESR spectra using a perturbational solution to the dipolar Hamiltonian: Teki, Y.; Takui, T.; Itoh, K. *J. Chem. Phys.* **1988**, *88*, 6134. Teki, Y.; Takui, T.; Yagi, H.; Itoh, K. *J. Chem. Phys.* **1985**, *83*, 539. Iwasaki, M. *J. Magn. Reson.* **1974**, *16*, 417.

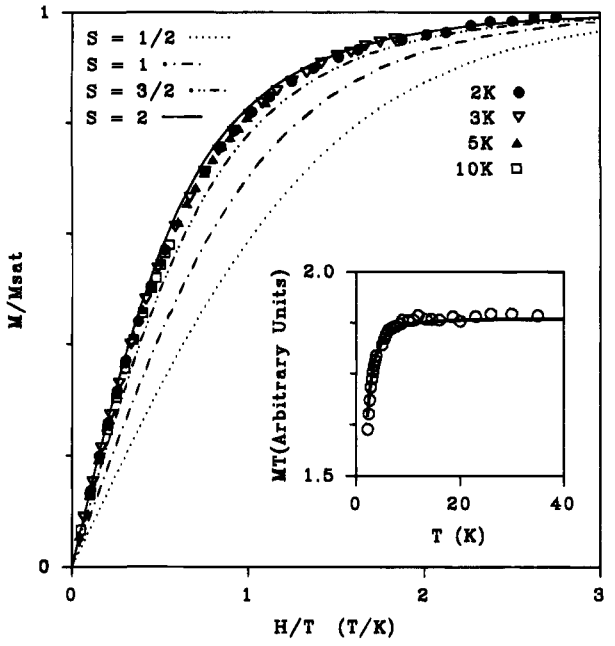

Figure 5. SQUID magnetometry of 2×10^{-3} M tetraradical **3**$^{4\bullet}$ in THF, which was obtained from **3**-$(OMe)_4$ using the Na/K alloy method. Main plot: M/M_{sat} vs H/T; solid circles, open triangles, solid triangles, and open squares correspond to experimental points at $T = 2$, 3, 5, 10 K, respectively. The solid line corresponds to the Brillouin function with $S = 2$. The fitting parameters at $T = 2$, 3, 5 K are $S = 1.86$, 1.87, 1.93, and $M_{sat} = 0.001\,44$, 0.001 44, 0.001 42; the parameter dependence is 0.43, 0.63, and 0.87, respectively. Insert plot: MT vs T at $H = 1.0$ T and fit with $S = 1.92$ and $M_{sat} = 0.001\,44$.

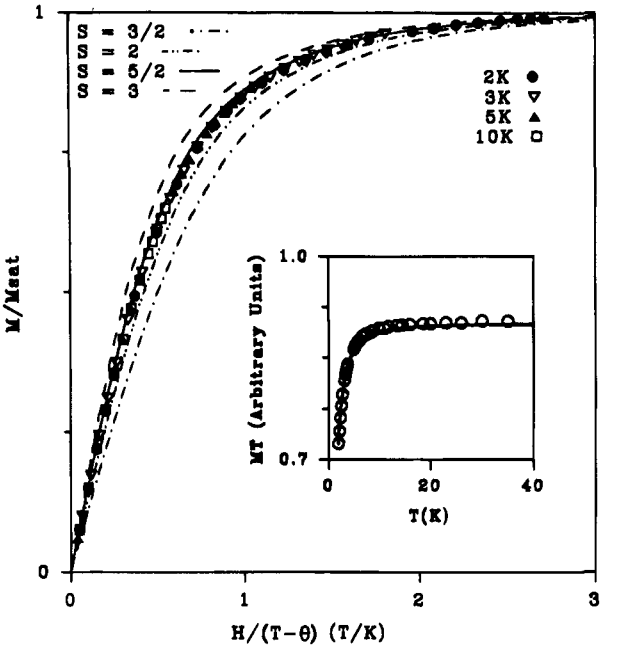

Figure 6. SQUID magnetometry of 9×10^{-3} M pentaradical **2**$^{5\bullet}$ in THF. Main plot: M/M_{sat} vs $H/(T - \theta)$, $\theta = -0.03$ K; solid circles, open triangles, solid triangles, and open squares correspond to experimental points at $T = 2$, 3, 5, 10 K, respectively. The solid line corresponds to the Brillouin function with $S = {}^5/_2$. The fitting parameters at $T = 2$, 3, 5 K are $S = 2.36$, 2.36, 2.37, and $M_{sat} = 0.005\,979$ at all T; the parameter dependence is 0.39, 0.58, and 0.81, respectively. Insert plot: MT vs T at $H = 1.0$ T and fit with $S = 2.36$, $M_{sat} = 0.005\,979$, and $\theta = -0.03$ K.

for **3**$^{4\bullet}$, which implies substantial signal intensity from an $S = 1$ state in both $\Delta m_s = 1$ and 2 regions of the ESR spectrum, may not be excluded.[15] This ambiguity could be resolved by magnetization studies.[1e,16]

Magnetization (M) is measured as a function of magnetic field ($H = 0-5.5$ T) and temperature ($T = 2-35$ K). For a dilute solution (2×10^{-3} M) of tetraradical **3**$^{4\bullet}$ in THF, which is obtained via the Na/K alloy method, M vs H data at $T = 2$, 3, 5, 10 K are fit (M vs H/T) to Brillouin functions with two variable parameters, S and magnetization at saturation, M_{sat} (Figure 5).[16] The values of S and M_{sat} fitted at each temperature are slightly different, e.g., S is in the range 1.86−1.93, with lower S corresponding to $T = 2$, 3 K; however, when a small correction with mean-field parameter, $\theta = -0.04$ K, i.e., H/T is replaced with $H/(T - \theta)$,[17] is introduced, the range of S narrows to 1.91−1.95.

The M vs T data ($T = 2.2-35$ K) are displayed as MT vs T; a Brillouin function with M_{sat}, obtained from the M vs H/T fit at $T = 2$ K, and $S = 1.92$ gives an adequate fit, except for a slight underestimate of the downward turn at low T (Figure 5, insert plot). Thus, some very small intermolecular (vide versa) antiferromagnetic interactions are still present in a 2×10^{-3} M solution of the tetraradical. The $S = 1.9$ is our best estimate for a sample of tetraradical **3**$^{4\bullet}$, which was obtained via the Na/K alloy method. Therefore, the $S = 2$ ground state is unambiguously established.

Magnetization studies of tetraradical **3**$^{4\bullet}$ in THF, which is generated from the tetraether using Li metal, confirm the above studies in two important aspects. First, the spin values are lower, $S = 1.8$, which suggests that the amount of low-spin impurities is about twice that of the samples obtained with the Na/K alloy, in accordance with ESR spectroscopy. Second, increase in concentration of the tetraradical results in greater antiferromagnetic interactions, with $0 < |\theta| \leq 0.3$ K ($\theta < 0$) for concentrations in the 1.8×10^{-3} to 1.3×10^{-2} M range, which is compatible with *intermolecular* interactions.

The lower values of S, compared to the theoretical $S = 2$ for the high-spin tetraradical, may be ascribed to the presence of defects. The samples with values of S close to the theoretical value are dominated by the tetraradical with zero and one defects when random distribution of defects is assumed. By the virtue of the macrocyclic connectivity, one defect merely converts the tetraradical to an $S = {}^3/_2$ triradical. Thus, the average $S = 1.9$ translates into the yield per arylmethyl site (p) for generation of an unpaired electron, $p \approx 0.95$ (95%), mixture containing ~80% of the $S = 2$ tetraradical and ~20% of the $S = {}^3/_2$ triradical (tetraradical with one defect). The presence of $S = 1$ or $^1/_2$ impurities would translate the average $S = 1.9$ into >80% content of the tetraradical.

(b) Pentaradical 2$^{5\bullet}$. Magnetization measurements for pentaradical **2**$^{5\bullet}$ in THF, which is prepared using the Li metal method, give at least $S \approx 2.3$ (Figure 6).[6] This is comparable (5−10% less than the theoretical value $S = {}^5/_2$) to tetraradical **3**$^{4\bullet}$. The ESR spectrum for pentaradical **2**$^{5\bullet}$ in 2-MeTHF/THF, which is prepared by the Na/K alloy method, consists of resonances in $\Delta m_s = 1$, 2, and 3 regions at $T = 4$ K (Figure 7).[18]

The $\Delta m_s = 1$ region consists of a narrow and intense center line, which is accompanied by six broad side lines. The intensity

(15) Berson, J. A. In *The Chemistry of Quinoid Compounds*; Patai, S., Rappaport, Z., Eds.; Wiley: 1988; Vol. II, Chapter 10.

(16) Brillouin function: Carlin, R. L. *Magnetochemistry*; Springer-Verlag: Berlin, 1986.

(17) Mean-field correction: Bino, A.; Johnston, D. C.; Goshorn, D. P.; Halbert, T. R.; Stiefel, E. I. *Science* **1988**, *241*, 1479.

(18) The ESR spectrum, which was reported in the preliminary communication (ref 6), was obtained at the liquid nitrogen temperature and, consequently, low signal-to-noise did not establish the presence of the resonances in the $\Delta m_s = 2$ and 3 regions.

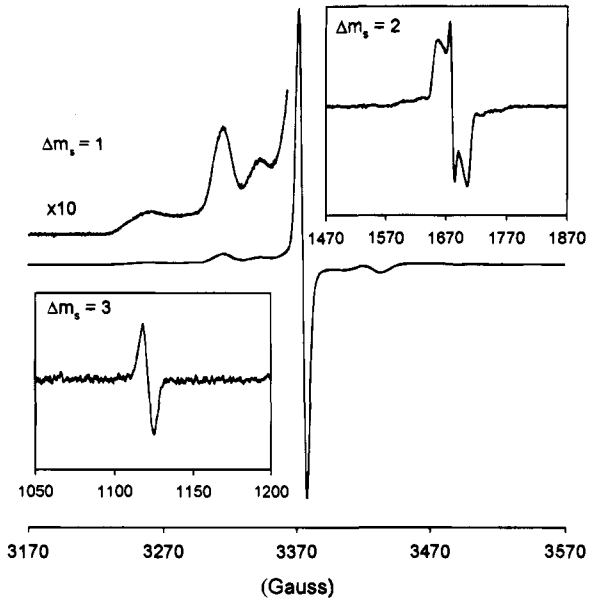

Figure 7. ESR spectrum for pentaradical $2^{5\bullet}$ in 2-MeTHF/THF at 4 K. The line shapes are somewhat distorted due to partial microwave saturation. Computer simulation (not shown) for the $\Delta m_s = 1$ region is compatible with a mixture of two $S = {}^5/_2$ systems with the following zfs: $|D/hc| = 0.0027$ cm^{-1}, $|E/hc| \approx 0$ cm^{-1} and $|D/hc| = 0.0027$ cm^{-1}, $|E/hc| = 0.0009$ cm^{-1}.

pattern precludes any single $S = {}^5/_2$ species; however, a mixture of two $S = {}^5/_2$ species with similar $|D/hc|$ but $E \approx 0$ and $E \approx D/3$ is compatible with the experimental spectrum. This is confirmed by computer simulation (not shown) for the $\Delta m_s = 1$ region,[14] which gives the following zfs parameters for the two $S = {}^5/_2$ states: $|D/hc| = 0.0027$ cm^{-1}, $|E/hc| \approx 0$ cm^{-1} and $|D/hc| = 0.0027$ cm^{-1}, $|E/hc| = 0.0009$ cm^{-1}. The relatively large peak height for the center line is also qualitatively reproduced by the simulation, as expected for half-integral S states.

The $\Delta m_s = 2$ region consists of a sharp center line, which is assigned to $S = 2$ or 1 impurities; the broad side lines are compatible with the $S = {}^5/_2$ states. The peak height and narrowness of the center line indicate only a small amount of impurities with integral S.

Detection of a resonance in the $\Delta m_s = 3$ region indicates the $S \geq {}^3/_2$ state, but for $2^{5\bullet}$, it is either the $S = {}^5/_2$ or ${}^3/_2$ state. (The broad side lines for $S = {}^5/_2$ are expected to have insufficient peak height and, possibly, line separation to be detectable at the present signal-to-noise and resolution.)

ESR spectroscopy indicates the dominant content of a half-integral S state, most likely, $S = {}^5/_2$, as a mixture of two conformers of pentaradical $2^{5\bullet}$. In conjunction with the measured $S \geq 2.3$ by SQUID magnetometry, the $S = {}^5/_2$ is the ground state.

(c) **Octaradical $1^{8\bullet}$.** All samples of octaradical $1^{8\bullet}$ are prepared using the Na/K alloy. Magnetization measurements in THF give $S = 3.8$,[6] which corresponds to $p \approx 0.95$ (95% per site or ~5% less than the theoretical value $S = 4.0$); thus, the p is similar to that for tetraradical $3^{4\bullet}$. Intermolecular antiferromagnetic interactions are negligible for 8×10^{-4} M $1^{8\bullet}$ in THF as indicated by the coincidence of the M vs H/T data at $T = 2$, 3, 5, 10 K; this allows for a two-parameter (S and M_{sat}) fit of M vs H/T to a Brillouin function. (The samples with higher concentration (~10^{-3} M) require a small correction for intermolecular antiferromagnetic interactions, $\theta < 0$ and $|\theta| \leq 0.1$ K.) Parameter dependencies at $T = 2$, 3, and 5 K are quite low (0.33, 0.45, and 0.67), indicating a reliable two-parameter fit. This lower parameter dependence, compared to the preceding pentaradical and tetraradical, originates in greater curvature of the M vs H/T plot for greater S.

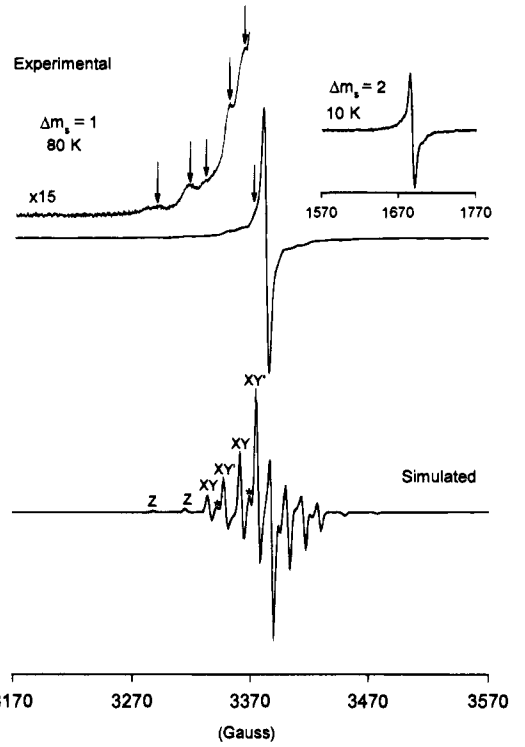

Figure 8. Experimental: ESR spectrum for octaradical $1^{8\bullet}$ in 2-MeTHF/THF, the $\Delta m_s = 1$ region at 80 K and the $\Delta m_s = 2$ region at 10 K. The arrows indicate approximate positions of the low-field six lines, which are labeled with letters in the simulation (Z, XY, XY'). Simulated: computer simulation for the $\Delta m_s = 1$ region of the $S = 4$ state with the following zfs, $|D/hc| = 0.00127$ cm^{-1} and $|E/hc| \approx 0$ cm^{-1}, and a Gaussian line width of 3 G. The two low-field inner Z lines, which are adjacent to the XY' lines, are labeled with asterisks; these Z lines are unresolved in the experimental spectrum.

The ESR spectrum in the $\Delta m_s = 1$ region for 8×10^{-4} M $1^{8\bullet}$ in 2-MeTHF/THF is poorly resolved (Figure 8), unlike the spectrum for $3^{4\bullet}$. There are two major factors to consider: (1) the same $p = 0.95$ corresponds to a much lower content of the defect-free octaradical compared to the defect-free tetraradical (~65% vs ~80%); (2) many more transitions for the octaradical compared to the tetraradical must fit into the similar ESR spectral width of the $\Delta m_s = 1$ region.[19] Point 2 implies ESR spectral congestion for $1^{8\bullet}$, as illustrated by the high-resolution (line width of 3.0 G) simulation of the $\Delta m_s = 1$ region of the ESR spectrum for the $S = 4$ octaradical (Figure 8). When the line width of the simulation is increased stepwise from 3 to 14 G, first, XY' lines envelope the four inner Z lines (labeled with an asterisk) and, then, the adjacent XY lines. In the experimental spectrum, the inner Z lines are not resolved and XY lines are somewhat less resolved than the XY' lines.

In spite of this qualitative agreement between the experimental and the simulated spectra, the substantial content of the half-integral S impurities (presumably, predominantly two $S = {}^7/_2$ octaradicals with one defect), as suggested by the dominant peak height of the center line, may distort the observed spectral pattern for the octaradical.[20]

(19) The ESR spectral width remains approximately constant for a series of homologous polyradicals because the D/hc may be related to the inverse of volume; ref 11.

(20) Conceivably, octaradicals with one defect at the inner or outer site of $1^{8\bullet}$ could be synthesized and, then, the ESR spectrum of $1^{8\bullet}$ might be simplified by spectral substraction of impurities with one defect.

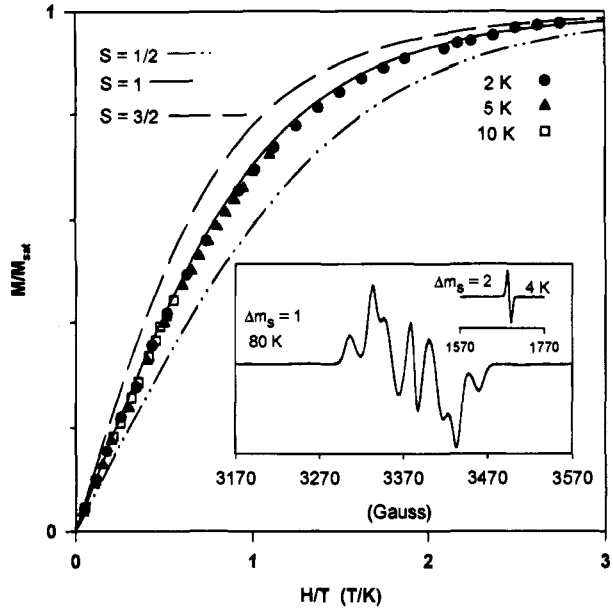

Figure 9. SQUID magnetometry and ESR spectroscopy of diradical **4-H²•**. Main plot: M/M_{sat} vs H/T for 3×10^{-3} M **4-H²•** in THF; solid circles, solid triangles, and open squares correspond to experimental points at $T = 2$, 5, 10 K, respectively. The parameter dependencies for fits with S and M_{sat} are 0.59 and 0.97 at $T = 2$ and 5 K, respectively. The solid line corresponds to the Brillouin function with $S = 1$. Insert plot: ESR spectrum for 3×10^{-3} M **4-H²•** in 2-MeTHF/THF at 80 K ($\Delta m_s = 1$ region) and 4 K ($\Delta m_s = 2$ region). Computer simulation (not shown) of the $\Delta m_s = 1$ region gives the following zfs parameters for an $S = 1$ state with $|D/hc| = 0.0072$ cm^{-1} and $|E/hc| = 0.0007$ cm^{-1}.

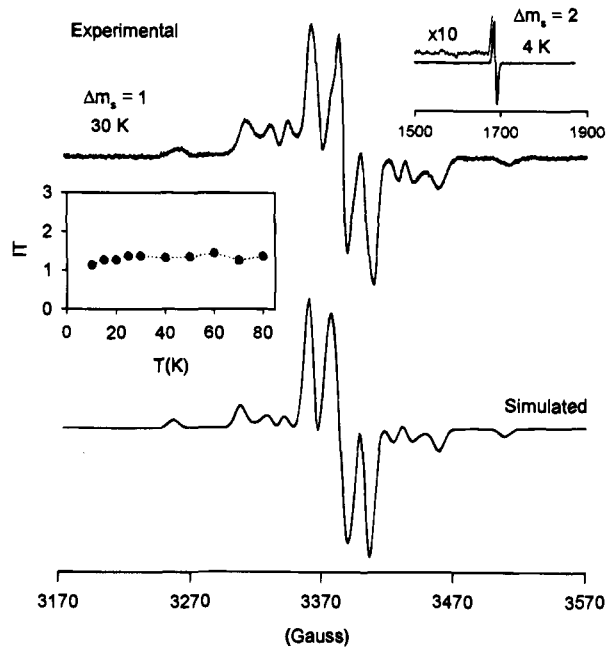

Figure 10. ESR spectroscopy of the dimer of triradical **4³•**. Experimental: $\Delta m_s = 1$ and 2 regions of the experimental spectrum in THF/2-MeTHF glass at 30 and 4 K, respectively; plot of the product (IT) of the intensity (I) for the $\Delta m_s = 2$ signal and the temperature (T) versus T. Simulated: simulation of the $\Delta m_s = 1$ region using second-order perturbation theory solution to the spin-only dipolar Hamiltonian for two (1:1) $S = 1$ spin systems with a Gaussian line width of 8 G and the following zfs parameters: $D/hc| = 0.0118$ cm^{-1}, $|E/hc| = 0.0008$ cm^{-1} and $|D/hc| = 0.0040$ cm^{-1}, $|E/hc| = 0$ cm^{-1}. A center line with a Gaussian line width of 15 G is added to account for the $S = {}^1/_2$ impurities.

The $\Delta m_s = 2$ region consists of an intense center line, with a broad base, which is consistent with the integral value $S \geq 2$. This resonance saturates much more readily than its $S = 2$ counterpart in **3⁴•**. The IT vs T plot for this signal is flat in the $T = 20-80$ K range. Both $\Delta m_s = 1$ and 2 regions show intense spectra at $T = 4$ K, though with distorted line shape due to microwave saturation.

In conjunction with the magnetization measurements, $S = 3.8$, for **1⁸•** and comprehensive characterization of **3⁴•**, it is concluded that **1⁸•** is the $S = 4$ ground state.

(d) Diradical 4-H²•. The ESR spectra for 3×10^{-3} M **4-H²•** in 2-MeTHF/THF in the 10−80 K range consist of an intense six-line pattern in the $\Delta m_s = 1$ region, which is reproduced by computer simulation as the $S = 1$ state with $|D/hc| = 0.0072$ cm^{-1} and $|E/hc| = 0.0007$ cm^{-1} (Figure 9).[21] In the 4−10 K range, an intense single line in the $\Delta m_s = 2$ region is observed (Figure 9); the $\Delta m_s = 1$ transitions are also very intense but their line shapes are somewhat distorted by microwave saturation at low temperatures. Magnetization studies of 3×10^{-3} M **4-H²•** in THF reveal an adequate fit (M vs H/T) to the Brillouin function with $S = 0.93$ at $T = 2$, 5, 10 K (Figure 9); the MT vs T plot is constant in the 2.2−15 K range, except for the saturation at the lowest T. These results establish unequivocally the $S = 1$ ground state for **4-H²•**.

(e) Dimer of Triradical 4³•. A yellow solution, which is obtained by oxidation of trianion **4³⁻,3Na(K)⁺** in THF and dilution with 2-MeTHF, as described above, shows a complex multiline pattern with the spectral width of ~200 G in the $\Delta m_s = 1$ region of X-band ESR spectra in the 10−120 K range (Figure 10). The relatively low intensity of the center peak indicates only a minor amount, if any, of a quartet state ($S = {}^3/_2$) triradical. (For a quartet state, $S = {}^3/_2$, triradical such as **4³•**, the peak height of the center line should be an order of magnitude greater than that of the side peaks.) The absence of any major amount of an $S = {}^3/_2$ triradical is further confirmed by the appearance of the $\Delta m_s = 2$ region, which consists of a single sharp peak in the 4−80 K range, and the failure to detect a $\Delta m_s = 3$ transition at 4 K.[11] The above ESR spectroscopic data are qualitatively consistent with a mixture of triplet ($S = 1$) diradicals. The $\Delta m_s = 1$ region of the experimental spectrum may be approximately reproduced as a 1/1 mixture of two $S = 1$ spin systems with the following zfs parameters: $|D/hc| = 0.0118$ cm^{-1}, $|E/hc| = 0.0008$ cm^{-1} and $|D/hc| = 0.0040$ cm^{-1}, $|E/hc| = 0$ cm^{-1} (Figure 10).[14]

The IT vs T plot for the $\Delta m_s = 2$ signal is approximately constant in the 20−80 K range, with a downward turn at lower temperature (Figure 10). A similar downward turn is found in the MT vs T plot for a sample of similar concentration in 2-MeTHF, using SQUID magnetometry; furthermore, M does not conform to the Brillouin function at low temperatures. The replacement of 2-MeTHF with THF in magnetization studies gives analogous behavior, except the onset of the downward turn is shifted to higher T. These results suggest the presence of weak antiferromagnetic interactions.[22]

As far as the structure of the dimer of **4³•** is concerned, one of the possilibities is the C−C bond formation between triarylmethyl and *para*/*ortho* (at the inner benzene ring) sites. This structure has its counterpart in the dimer of Gomberg's triphenylmethyl and it is consistent with the two $S = 1$ diradicals, which have the ratio of their D values approximately equal to 3.[23,24] Such structure also suggests similarity between

(21) An ESR spectrum for the $S = 2$ state for a calix[3]arene-based dicarbene, analogous to **4-H²•**, is mentioned in ref 1c.

(22) Concentration-dependence studies are inconclusive as to whether these antiferromagnetic interactions are intra- or intermolecular.

the diradical in the dimer with the greater $|D/hc|$ and the model diradical **4-H$^{2\bullet}$**; however, their D values are quite different. The dimer C−C bond undergoes readily reductive cleavage; the quenching products **4-(X)$_3$** (X = H, D) are isolated in good yields. An attempt to prepare the triradical **4$^{3\bullet}$** by oxidation of **4^{3-},3Na(K)$^+$** in Me_2O at 150 K is hampered by slow reaction at low temperature; following the dilution with 2-MeTHF, the ESR spectrum at 80 K is similar to that in Figure 10, though the peak height of the center line is greater by a factor of >2.

Conclusion

Studies of calix[3]arene-based diradical and triradical suggest synthesis of high-spin polyradicals, based on this macrocycle, such as the Mataga polymer, may be difficult. The dimerization of the calix[3]arene-based triradical may reflect insufficient steric hindrance in this relatively planar system compared to its calix[4]arene-based tetraradical counterpart.[25]

Calix[4]arene-based polyradicals, which have their π-conjugated system twisted out-of-plane, may be an ideal compromise. The distortion is large enough to provide steric protection for the kinetic stability but still moderate to preserve the ferromagnetic spin coupling (high-spin ground states). Therefore, calix[4]arene-based macrocyclic polyradicals are viable building blocks for defect-resilient high-spin polyradicals. The synthesis of the larger calix[*n*]arene macrocycles and annelated 2-strand calix[4]arenes is being undertaken in our laboratories.[1e]

Experimental Section

Materials. Ether and tetrahydrofuran (THF) for use on vacuum lines were distilled from sodium/benzophenone in a nitrogen atmosphere. Iodine (99.999%, resublimed crystals) was provided by Johnson-Mathey and 3-bromo-4′-*tert*-butylbenzophenone was prepared as described previously.[26] Other major chemicals were obtained from Aldrich.

Special Procedures. Solutions of carbopolyanions in THF (or ether) were prepared in a Vacuum Atmospheres glovebox; outside the glovebox, carbopolyanions were handled on a 10^{-3} Torr vacuum line.[10] Similar vacuum lines were used for all air-sensitive synthetic procedures.

NMR Spectroscopy and Other Analyses. NMR spectra were obtained using Omega spectrometers (^{1}H, 500 and 300 MHz) in $CDCl_3$ and THF-d_8; the chemical shift references were ^{1}H, TMS, 0.0 ppm and ^{13}C, $CDCl_3$, 77.0 ppm in $CDCl_3$ and ^{1}H, THF-d_7, 3.580 ppm and ^{13}C, THF-d_8, 67.45 ppm. ^{6}Li and ^{7}Li NMR spectra were obtained on the 500 MHz instrument at 73.6 and 194.4 MHz, respectively. IR spectra were obtained as described previously.[3] Voltammetry data were obtained, in a glovebox, at 200 K, as described elsewhere;[11] 100-μm Pt-disk electrodes were used. Elemental analyses were completed by Dr. G. M. Dabkowski (Director-Microanalytics, P.O. Box 199, So. Deerfield, MA 01373).

Alcohol 5-OH and Ether 5-OMe. *n*-BuLi (15.2 mL of a 2.5 M solution in hexane, 38.0 mmol) was added to a solution of 1,3-dibromobenzene (8.970 g, 38.02 mmol) in ether (125 mL) at −78 °C. After 20 min at −78 °C, 3-bromo-4′-*tert*-butylbenzophenone (12.00 g, 37.85 mmol) in ether (75 mL) was added to the reaction mixture at −78 °C. The temperature in the cooling bath was allowed to rise to −15 °C over a period of 80 min; subsequently, the reaction mixture was quenched with water (75 mL). After extraction with ether (2 × 250 mL), the combined organic layer was washed with water (1 × 100 mL) and brine (1 × 100 mL) and, then, dried over $MgSO_4$. Concentration in vacuo gave 18.07 g of light yellow viscous liquid. Column chromatography (silica, hexane/EtOAc, from 13/1 to 7/1) afforded alcohol **5-OH** (17.26 g), which is suitable for use in the next step in the synthesis.

A 1-L flask with a sidearm was charged with NaH (7.2 g of 60% dispersion in mineral oil, 0.18 mol). After removal of mineral oil with pentane (3 × 60 mL) under nitrogen flow, THF (250 mL) was added and, then, during cooling with an ice bath, alcohol **5-OH** (10.20 g, 21.50 mmol) in THF (100 mL) was added. The resultant suspension was stirred for 5 h during which time the temperature of cooling bath was allowed to reach ~10 °C. After the bath was recooled to 0 °C, MeI (18.8 mL, 0.300 mol) was added. The reaction mixture was stirred at ambient temperature for 15 h and, then, poured over cold water (200 mL) in a separatory funnel. Aqueous workup analogous to that described above for **5-OH** gave 10.67 g of yellow solid, which when recrystallized from MeOH/ether afforded 9.120 g (86%) of white solid (mp 104−106 °C). Anal. Calcd for $C_{24}H_{24}OBr_2$: C, 59.04; H, 4.95. Found: C, 59.29; H, 4.82. ^{1}H NMR ($CDCl_3$): 7.64 (t, J = 2, 2 H), 7.40−7.13 (m, 10 H), 3.03 (s, 3 H), 1.32 (s, 9 H). {^{1}H}^{13}C NMR ($CDCl_3$): 150.5, 146.5, 138.4, 131.1, 130.2, 129.4, 128.8, 127.2, 124.9, 122.2, 86.1, 52.1, 34.5, 31.3. FABMS (ONPOE), cluster: *m/z* (peak height) at M^+, 488.1 (1); $(M - OCH_3)^+$, 455.0 (5.5), 456.0 (1.5), 457.0 (10), 458.0 (3), 459.0 (5), 460.0 (1.5).

Hydrocarbon 5-H. Trifluoroacetic acid (65 mL) was added to a solution of ether **5-OMe** (3.50 g, 7.17 mmol) in dichloromethane (65 mL) at 0 °C. To the resultant orange/red solution, 10 pellets of sodium borohydride (multimolar excess) were slowly added. The reaction mixture became colorless and, after overnight stirring, TLC analysis showed disappearance of **5-OMe**. The reaction mixture was poured into cold water, neutralized with KOH pellets to pH ≈ 7, and extracted with ether (2 × 200 mL). The combined ether extracts were washed with dilute KOH_{aq}, water, and brine. After drying over $MgSO_4$ and filtration, removal of the solvents in vacuo gave crude product (3.39 g). Filtration through a bed of silica gel gave **5-H** (3.15 g). ^{1}H NMR (500 MHz, $CDCl_3$): 7.36 (bd, J = 7, 2 H), 7.31 (d, J = 8, 2 H), 7.26 (t, J = 2, 2 H), 7.16 (t, J = 8, 2 H), 7.02 (bd, J = 7, 2 H), 6.98 (d, J = 8, 2 H), 5.41 (s, 1 H), 1.31 (s, 9 H). {^{1}H}^{13}C NMR (125 MHz, $CDCl_3$): 149.7, 145.7, 139.1, 132.3, 129.9, 129.7, 128.8, 128.0, 125.5, 122.7, 55.8, 34.4, 31.3.

Diketone 6. *t*-BuLi (12.0 mL of a 1.7 M solution in pentane, 20.4 mmol) was added to a solution of ether **5-OMe** (2.44 g, 5.00 mmol) in THF (150 mL) at −78 °C. After 15 min at −78 °C, 1-(4-*tert*-butylbenzoyl)pyrrolidine (2.77 g, 12.0 mmol) in THF (50 mL) was added. The reaction mixture was allowed to warm up to ambient temperature overnight. After being quenched with water (50 mL) and extracted with ether (2 × 250 mL), the combined organic phase was washed with water (150 mL) and brine (150 mL) and, then, dried over $MgSO_4$. Filtration, concentration in vacuo, and column chromatography (silica, hexane/EtOAc, from 32/1 to 9/1) afforded 2.77 g of white solid. Subsequent recrystallization from MeOH/ether (9/1) gave 2.34 g (73%) of white powder (mp 162−164 °C). ^{1}H NMR ($CDCl_3$): 7.90 (bs, 2 H), 7.76−7.66 (m, 8 H), 7.48−7.40 (m, 6 H), 7.34 (bs, 4 H), 3.07 (s, 3 H), 1.33 (s, 18 H), 1.32 (s, 9 H). {^{1}H}^{13}C NMR ($CDCl_3$): 196.0, 156.2, 150.3, 144.5, 139.0, 137.5, 134.5, 132.0, 130.2, 129.9, 128.8, 128.7, 128.0, 125.2, 124.9, 86.5, 52.1, 35.0, 34.4, 31.3, 31.0. IR (cm^{-1}): 1656 (C=O), 1605 (ArH). Anal. Calcd for $C_{46}H_{50}O_3$: C, 84.88; H, 7.74. Found: C, 84.58; H, 7.93. FABMS (3-NBA/Na_2CO_3), cluster: *m/z* (peak height) at $(M + Na)^+$, 673.3 (0.5); $(M + H)^+$, 651.3 (1), 652.3 (0.5); $(M - OCH_3)^+$, 619.2 (4), 620.3 (2).

Diether−Diol 3-(OMe)$_2$(OH)$_2$. *t*-BuLi (1.18 mL of a 1.7 M solution in pentane, 2.01 mmol) was added to a solution of ether **5-OMe** (0.244 g, 0.500 mmol) in THF (25 mL) at −78 °C. After 15 min at −78 °C, diketone **6** (0.325 g, 0.500 mmol) in THF (15 mL) was added. The reaction mixture was allowed to warm up to ambient temperature over 12 h and, then, was further stirred for 36 h. After being quenched with water (10 mL) and extracted with ether (2 × 100 mL), the combined organic phase was washed with water (50 mL) and brine (50 mL) and, then, dried over $MgSO_4$. Filtration, concentration in vacuo, and column chromatography (silica, hexane/EtOAc, from 32/1 to 9/1) afforded 0.171 g (35%) of white powder (mp 136−174 °C), which appears to be mixture of isomers **3-(OMe)$_2$(OH)$_2$**. The yield is 26%, when the reaction is scaled up three times. ^{1}H NMR ($CDCl_3$):

(23) Lankamp, H.; Nauta, W. T.; MacLean, C. *Tetrahedron Lett.* **1968**, 249. Gomberg, M. *J. Am. Chem. Soc.* **1900**, *22*, 757.

(24) The diradical with the smaller D-value in the dimer may be considered as union triarylmethyl and arylpentadienyl-like monoradicals. Thus, the spin density will be only ~1/3 at the two previous triarylmethyl sites compared to the larger D-value diradical.

(25) Sabacky, M. J.; Johnson, C. S., Jr.; Smith, R. G.; Gutowsky, H. S.; Martin, J. C. *J. Am. Chem. Soc.* **1967**, *89*, 2054.

(26) Rajca, A. *J. Org. Chem.* **1991**, *56*, 3557.

7.30–6.45 (m, 32 H), 2.9–2.5 (8 H), 1.25–1.15 (5 peaks, 36 H). $\{^1H\}^{13}C$ NMR ($CDCl_3$): 150–140 (16 peaks), 130–124 (21 peaks), 86.8, 82.2–81.9 (4 peaks), 52–51 (3 peaks), 34.4, 31.34, 31.30. IR (cm^{-1}): 3500 (OH), 1600 (ArH). FABMS (3-NBA/Na_2CO_3), cluster: *m/z* (peak height) at $(M - OH)^+$, 963.4 (9), 964.4 (6.5), 965.4 (3); $(M - OCH_3)^+$, 949.4 (10), 950.4 (7), 951.4 (3).

Ether–Diol 4-OMe-(OH)$_2$. *t*-BuLi (11.8 mL of a 1.7 M solution in pentane, 20.1 mmol) was added to a solution of ether **5-OMe** (2.44 g, 5.00 mmol) in THF (300 mL) at −78 °C. After 20 min at −78 °C, 1,3-phenylenebis(4-*tert*-butylphenyl)methanone (1.99 g, 5.00 mmol) in THF (75 mL) was added. The reaction mixture was allowed to warm up to ambient temperature over 17 h. After being quenched with water (50 mL) and extracted with ether (2 × 300 mL), the combined organic phase was washed with water (150 mL) and brine (2 × 100 mL) and, then, dried over $MgSO_4$. Filtration, concentration in vacuo, and column chromatography (silica, hexane/EtOAc, from 19/1 to 4/1) afforded two isomers **4-OMe-(OH)$_2$**: Less and more polar isomers were identified as *trans* and *cis* diol isomers, respectively. Only the *trans* isomer was isolated analytically pure.

(a) *Trans* Diol Isomer (0.853 g, 23%, mp 210–211 °C). Anal. Calcd for $C_{52}H_{56}O_3$: C, 85.67; H, 7.74. Found: C, 85.49; H, 8.04. ^1H NMR ($CDCl_3$): 7.52–7.02 (m, 22 H), 6.96 (bs, 1 H), 6.81 (bs, 1 H), 3.09 (s, 3 H), 2.62 (s, 1 H), 2.51 (s, 1 H), 1.33 (s, 18 H), 1.31 (s, 9 H). $\{^1H\}^{13}C$ NMR ($CDCl_3$): 150.16 (overlap), 150.06, 147.8, 147.0, 146.83, 146.79, 144.8, 143.8, 142.0, 141.7, 138.9, 132.1, 131.17, 131.08, 128.8, 128.0, 127.6, 127.5, 127.3, 127.1, 126.8, 126.4, 126.0, 125.4, 125.0 (overlap), 124.9, 124.1, 124.0, 87.9, 82.30, 82.23, 52.1, 34.5, 31.3. IR (cm^{-1}): 3600, 3500 (OH), 1600 (ArH). FABMS (3-NBA/Na_2CO_3), cluster: *m/z* (peak height) at $(M - OH)^+$, 711.3 (10), 712.3 (6), 713.3 (3); $(M - OCH_3)^+$, 697.3 (6), 698.3 (3).

(b) *Cis* Diol Isomer (0.748 g, 20%, sufficient purity for the next step in the synthesis). Because of impurity peaks, NMR spectral assignments are tentative. ^1H NMR ($CDCl_3$): 7.5–6.7 (m, 24 H), 3.08 (s, 3 H), 2.53 (s, 2 H), 1.34 (s, 27 H). $\{^1H\}^{13}C$ NMR ($CDCl_3$): 150.4, 150.0, 147.41, 147.38, 145.1, 141.9, 138.1, 131.7, 131.4, 129.5, 127.6, 127.5, 127.4, 127.2, 126.0, 124.95, 124.91, 124.7, 124.6, 88.0, 82.2, 52.2, 34.5, 31.3. FABMS (3-NBA/Na_2CO_3), cluster: *m/z* (peak height) at $(M - OH)^+$, 711.3 (10), 712.3 (6), 713.3 (2); $(M - OCH_3)^+$, 697.3 (7), 698.3 (3).

Diol 4-H-(OH)$_2$. The procedure analogous to that for **4-OMe-(OH)$_2$** was followed, using **5-H** (3.00 g, 6.55 mmol) in THF (100 mL), *t*-BuLi (15.4 mL, 26.2 mmol), and 1,3-phenylenebis(4-*tert*-butylphenyl)-methanone (2.61 g, 6.55 mmol). Column chromatography (flash silica, ether in hexane, from 5% to 13%), afforded two isomers of **4-H-(OH)$_2$** as pale yellow solids (yield, 52%); only the *trans* isomer was fully characterized.

***Trans* Diol Isomer** (1.533 g, 36%). ^1H NMR ($CDCl_3$): 7.49 (bd, $J = 7$, 1 H), 7.45–7.00 (m, 20 H), 6.89 (bs, 1 H), 6.80 (bs, 1 H), 6.68 (bd, $J = 7$, 1 H), 5.40 (s, 1 H), 2.51 (s, 1 H), 2.48 (s, 1 H), 1.33 (s, 9 H), 1.32 (s, 9 H), 1.31 (s, 9 H). $\{^1H\}^{13}C$ NMR (125 MHz, $CDCl_3$): 150.4, 150.3, 149.3, 147.7, 147.6, 147.3, 147.0, 144.2, 143.9, 142.2, 141.9, 139.7, 131.3, 131.2, 130.9, 129.0, 128.4, 128.1, 127.7, 127.5, 127.4, 125.7, 125.4, 125.2, 125.1, 123.9, 123.8, 82.43, 82.40, 56.2, 34.5, 34.4, 31.40, 31.36, 31.33. FABMS (ONPOE), cluster: *m/z* (peak height) at M^+, 697.4 (1.5), 698.4 (2), 699.4 (1); $(M - OH)^+$, 680.4 (<1), 681.4 (10), 682.4 (5.5), 683.4 (2).

Tetraether 3-(OMe)$_4$. A 100-mL flask with a sidearm was charged with NaH (0.30 g of 60% dispersion in mineral oil, 7.5 mmol). After removal of the mineral oil with pentane (3 × 15 mL) under nitrogen flow, THF (40 mL) was added and, then, during cooling with an ice bath, diether–diol **3-(OMe)$_2$(OH)$_2$** (0.320 g, 0.326 mmol) in THF (20 mL) was added. The resultant suspension was stirred for 6 h during which time the temperature of the cooling bath was allowed to reach ambient temperature. After the bath was recooled to 0 °C, MeI (1.50 mL, 24.0 mmol) was added. The stirred reaction mixture was allowed to attain ambient temperature over 3 h and, then, it was stirred for 10 h. Pouring the mixture over cold water (25 mL) in a separatory funnel was followed by the usual aqueous workup. Purification with column chromatography (silica, from 2% to 6% EtOAc in hexane) gave 0.232 g of a white solid and, after crystallization from MeOH, 0.184 g (56%) of a white powder (mp 152–162 °C). ^1H NMR ($CDCl_3$): 7.35–7.05 (m, 32 H), 2.98–2.88 (four peaks, 12 H), 1.30–1.28 (four peaks, 36 H). $\{^1H\}^{13}C$ NMR ($CDCl_3$): 150–140 (11 peaks), 130–124 (16 peaks), 87.5–86.5 (3 peaks), 52.5–52.0 (2 peaks), 34.3, 31.3. IR (cm^{-1}): 1600 (ArH). Anal. Calcd for $C_{72}H_{80}O_4$: C, 85.71; H, 7.92. Found: C, 85.93; H, 8.48. FABMS (3-NBA), cluster: *m/z* (peak height) at $(M - OCH_3)^+$, 977.6 (10), 978.6 (8), 979.6 (3).

Triether 4-(OMe)$_3$. (a) *Trans* Isomer. A 100-mL flask with a sidearm was charged with NaH (0.656 g of 60% dispersion in mineral oil, 16.4 mmol). After removal of the mineral oil with pentane (3 × 25 mL) under nitrogen flow, THF (60 mL) was added and, then, during cooling with an ice bath, *trans* ether–diol **4-OMe-(OH)$_2$** (0.500 g, 0.686 mmol) in THF (20 mL) was added. The resultant suspension was stirred for 5 h during which time the temperature of the cooling bath was allowed to reach ambient temperature. After the bath was recooled to 0 °C, MeI (3.60 mL, 57.8 mmol) was added. The reaction mixture was stirred at ambient temperature for 16 h and, then, poured over cold water (75 mL) in a separatory funnel. Aqueous workup gave 0.510 g of crude product, which upon recrystallization from MeOH afforded 0.292 g (56%) of white powder (mp 194–197 °C). Anal. Calcd for $C_{54}H_{60}O_3$: C, 85.67; H, 7.99. Found: C, 86.03; H, 8.37. ^1H NMR ($CDCl_3$): 7.46–7.14 (m, 21 H), 7.03 (br s, 2 H), 6.89 (br s, 1 H), 3.16 (s, 3 H), 3.09 (s, 6 H), 1.31 (s, 18 H), 1.28 (s, 9 H). $\{^1H\}^{13}C$ NMR (125 MHz, $CDCl_3$): 149.8, 145.2, 144.0, 143.0, 140.1, 139.8, 133.7, 132.0, 128.1 (overlap), 127.6, 127.1, 127.0, 126.3, 124.76, 124.73, 124.1, 87.7 (overlap), 52.4, 52.3, 34.4, 31.4. IR (cm^{-1}): 1600 (ArH). FABMS (3-NBA), cluster: *m/z* (peak height) at M^+, 757.5 (1), 756.5 (1); $(M - OCH_3)^+$, 725.5 (10), 726.5 (6), 727.5 (2).

(b) *Cis* Isomer. The crude product was obtained from *cis* ether–diol **4-OMe-(OH)$_2$** (0.500 g) similarly to the *trans* isomer. Purification by column chromatography (silica, hexane/EtOAc, from 49:1 to 16:1) gave 0.327 g (63%) of a white solid; crystallization from MeOH gave 0.221 g (43%) of a white powder (mp 250–251 °C). ^1H NMR ($CDCl_3$): 7.4–7.1 (m, 21 H), 6.98 (br s, 3 H), 3.02 (s, 9 H), 1.33 (s, 27 H). $\{^1H\}^{13}C$ NMR (125 MHz, $CDCl_3$): 149.9, 143.9, 140.5, 133.4, 128.1 (br), 127.4, 125.3, 124.6, 87.6, 52.2, 34.4, 31.4. FABMS (3-NBA), cluster: *m/z* (peak height) at M^+, 757.5 (1), 756.5 (1); $(M - OCH_3)^+$, 725.5 (10), 726.5 (6), 727.5 (2).

Diether 4-H-(OMe)$_2$. The procedure analogous to that used for triether **4-(OMe)$_3$** was followed, using the *trans* isomer of diol **4-H-(OH)$_2$** (1.03 g, 1.47 mmol) in THF (45 mL), NaH (1.42 g of 60% dispersion in mineral oil, 35.4 mmol), and MeI (7.8 mL, 0.12 mol). Recrystallization (precipitation) from ether/MeOH gave 0.459 g (43%) of analytically pure product as a white solid (mp 150–160 °C, glass-like). ^1H NMR (500 MHz, $CDCl_3$): 7.45–7.05 (m, 20 H), 7.00 (bd, $J = 7$, 1 H), 6.84 (bs, 1 H), 6.73 (bs, 1 H), 6.62 (bd, $J = 7$, 1 H), 5.42 (s, 1 H), 3.14 (s, 3 H), 3.11 (s, 1 H), 1.311–1.299 (3 singlets, 1/1/1, 27 H). $\{^1H\}^{13}C$ NMR/DEPT (125 MHz, $CDCl_3$): aromatic quaternary region, expected, 12 resonances; found, 11 resonances at 150.0 (q), 149.8 (q), 149.2 (q), 145.8 (q), 145.3 (q), 144.9 (q), 144.1 (q), 143.0 (q), 139.7 (q), 139.6 (q), 138.8 (q); aromatic nonquaternary region, expected, 18 resonances; found, 18 resonances at 133.6, 132.0, 131.7, 129.0, 128.7, 128.3, 128.1, 127.7, 127.5, 127.1, 127.0, 126.6, 125.5, 125.4, 124.81, 124.76, 124.3, 124.0; nonaromatic region, 87.8 (q), 87.7 (q), 55.9, 52.2, 34.4 (q), 31.4, 31.3. Anal. Calcd for $C_{53}H_{58}O_2$: C, 87.56; H, 8.04. Found: C, 87.40; H, 7.89. FABMS (ONPOE), cluster: *m/z* (peak height) at M^+, 725.4 (1), 726.4 (2), 227.4 (1.5); $(M - OCH_3)^+$, 694.4 (1), 695.4 (10), 696.4 (6), 697.4 (1.5).

Carbotetraanion 3^{4-}: NMR Spectroscopy and Quenching Products 3-D$_4$. (1) MeOD Quenching. Tetraether (10.1 mg) was stirred with excess Li metal in THF (0.5 mL) in a glovebox for 3 days. The resultant red reaction mixture in a rubber/Teflon capped vial was placed on a vacuum line under nitrogen and, then, MeOD (0.3 mL) was added. The light yellow reaction mixture was transferred to ether (50 mL) where the usual aqueous workup gave crude product. ^1H NMR ($CDCl_3$): 7.75–7.50 (m, impurities, <5% of aromatic region), 7.40–6.50 (m, aromatic region), 5.42–5.32 (3–4 peaks, 0.2 H), 1.35–1.30 (bs). Subsequent separation by PTLC (Analtech silica, hexane/ether, 98/2) produced isomeric products: less polar spot, ^1H NMR ($CDCl_3$): 7.30–6.85 (m, 28 H), 6.56–6.51 (m, 4 H), 1.30 (bs, 36 H); FABMS (3-NBA), cluster: *m/z* (peak height) at $M^+/(M + H)^+$, 890.6 (6.5), 891.6 (7), 892.6 (9.5), 893.6 (10), 894.6 (5.5), 895.6 (2); more polar spot, ^1H NMR ($CDCl_3$): 7.30–6.84 (m, 28 H), 6.61 (bm, 2 H), 6.54 (bm, 2 H), 1.32–1.30 (36 H), FABMS (ONPOE), cluster: *m/z* (peak

height) at $M^+/(M + H)^+$, 890.6 (4), 891.6 (5), 892.6 (10), 893.6 (10), 894.6 (5.5), 895.6 (2).

(2) NMR Spectroscopy. ^1H NMR (500 MHz, THF-d_8): 293 K, 6.975 (d, $J = 9$, 8 H), 6.542 (s, 4 H), 6.442 (d, $J = 8-9$, 16 H), 6.354 (t, $J = 8$, 4 H), 1.130 (s, 36 H); 250 K, EM = −1.3 Hz, GB = +0.7 Hz, 6.97 (d, $J = 9$, 8 H), 6.47 (d of d, $J = 8$, $J = 2$, 8 H), 6.45 (t, $J = 2$, 4 H), 6.35 (d, $J = 9$, 8 H), 6.31 (t, $J = 8$, 4 H), 1.11 (s, 36 H); 230 K, EM = −1.5 Hz, GB = +0.7 Hz, 6.96 (d, $J = 9$, 8 H), 6.47 (d of d, $J = 8$, $J = 2$, 8 H), 6.41 (t, $J = 2$, 4 H), 6.32 (d, $J = 9$, 8 H), 6.29 (t, $J = 8$, 4 H), 1.10 (s, 36 H); 210 K, 6.95 (d, $J = 8$, 8 H), 6.46 (d, $J = 7$, 8 H), 6.36 (s, 4 H), 6.30−6.25 (m, 12 H), 1.10 (s, 36 H); 190 K, 6.95 (bs, 8 H), 6.44 (bs, 8 H), 6.33 (s, 4 H), 6.30−6.25 (m, 12 H), 1.10 (s, 36 H); 178 K, 7.5−6.0 (broad hump with relatively sharp multiplet at 6.30−6.25), 1.09 (s). $\{^1H\}^{13}C$ NMR (125 MHz, THF-d_8): 293 K, 150.1, 147.4, 129.6, 127.8, 125.8, 124.2, 120.5, 115.2, 83.4, 33.9, 32.3; 210 K, 150.3, 147.5, 127.3, 126.9, 126.4, 123.9, 119.3, 116.1, 83.5, 33.8, 32.4. ^6Li NMR (THF-d_8): 178 K, singlet, $\Delta\nu_{1/2} = 2$ Hz. ^7Li NMR (THF-d_8): 178 K, singlet, $\Delta\nu_{1/2} = 14$ Hz.

Carbotrianion 4^{3-},3Na(K)$^+$: NMR Spectroscopy and Quenching Products 4-D_3. (1) MeOD Quenching. A drop of Na/K alloy was added to a stirred THF (0.5 mL) solution of triether (6.6 mg) in a glovebox; a red color appeared immediately. After 2 days of stirring in a rubber/Teflon septum capped vial, the reaction mixture was placed on a vacuum line under a stream of nitrogen or argon and MeOD (0.3 mL) was added. The light yellow reaction mixture was transferred to ether (50 mL) and subjected to the usual aqueous workup. ^1H NMR ($CDCl_3$): ^1H NMR ($CDCl_3$): 7.40−6.65 (m, 24 H), 5.50−5.30 (three singlets, <0.2 H), 1.35−1.30 (three singlets at 1.33, 1.32, 1.30; 2/2/1; 27 H). Separation by PTLC (silica, hexane/ether, 98/2) gave two isomers: the less polar (*trans* isomer), ^1H NMR ($CDCl_3$): 7.36−6.87 (m, 22 H), 6.69 (bd, $J = 8$, 2 H), 5.30−5.50 (two singlets at 5.38 and 5.35, <0.2 H), 1.32 (s, 18 H), 1.30 (s, 9 H). FABMS (ONPOE), cluster: *m/z* (peak height) at $M^+/(M + H)^+$, 667.4 (4), 668.4 (5), 669.4 (10), 670.4 (9), 671.4 (4); the more polar (*cis* isomer), ^1H NMR ($CDCl_3$): 7.38−6.82 (m, 24 H), 5.31 (s, <0.1 H), 1.33 (s, 27 H). FABMS (ONPOE), cluster: *m/z* (peak height) at $M^+/(M + H)^+$, 667.5 (4.5), 668.5 (4.5), 669.5 (10), 670.5 (10), 671.5 (5).

(2) NMR Spectroscopy. In an evacuated vessel, which possessed a sidearm NMR tube connected to the reaction compartment via a fine glass frit, triether (*trans* isomer, 17 mg) was stirred in THF-d_8 (0.6 mL) with a drop of Na/K alloy. After 6 days, the deep red reaction mixture was filtered to the NMR tube under argon pressure and, then, the tube was evacuated at −95 °C and flame sealed. Less concentrated sample: ^1H NMR (500 MHz, THF-d_8): 293 K, 3-fold-symmetric isomer, 7.142 (d, $J = 8$, 6 H, C), 7.062 (bs, 3 H, C′1), 6.650 (d of d, $J = 8$, $J = 1.5$, 6 H, C′2), 6.622 (d, $J = 8$, 6 H, C), 6.307 (t, $J = 8$, 3 H, C′3), 1.173 (s, 27 H), 2-fold-symmetric isomer, 7.377 (d, $J = 8$, 2 H, A), 7.275 (d, $J = 8$, 4 H, B), 7.238 (bd, $J = 8$, 2 H, B′2), 7.192 (d, $J = 8$, 2 H, A), 7.169 (bs, 2 H, B′1), 7.062 (bs, 1 H, A′1), 6.676 (d, $J = 8$, 4 H, B), 6.394 (d of d, $J = 8$, $J = 7$, 2 H, B′3), 6.336 (d of d, $J = 8$, $J = 1.5$, 2 H, A′2), 6.189 (t, $J = 8$, 1 H, A′3), 5.910 (bd, $J = 7$, 2 H, B′2), 1.277 (s, 9 H), 1.182 (s, 18 H). More concentrated sample: ^1H NMR (500 MHz, THF-d_8): δ ($^1H-^1H$ COSY cross-peak, assignment) 293 K, 3-fold-symmetric isomer, 7.163 (d, $J = 8$, 6 H, 6.639, C), 7.113 (bs, 3 H, 6.664, C′1), 6.664 (d, $J = 8$, 6 H, 7.113/6.330, C′2), 6.639 (d, $J = 8$, 6 H, 7.163, C), 6.330 (t, $J = 8$, 3 H, 6.639, C′3), 1.176 (s, 27 H), 2-fold-symmetric isomer, 7.381 (d, $J = 8$, 2 H, 7.193, A), 7.277 (d, $J = 8$, 4 H, 6.681, B), 7.238 (d, $J = 8$, 2 H, 6.396/7.171/5.913, B′2), 7.193 (d, $J = 8$, 2 H, 7.381, A), 7.171 (bs, 2 H, 7.238/5.913, B′1), 7.129 (bs, 1 H, 6.338, A′1), 6.681 (d, $J = 8$, 4 H, 7.277, B), 6.396 (t, $J = 8$, 2 H, 7.238/5.913, B′3), 6.338 (d, $J = 8$, 2 H, 6.193/7.129, A′2), 6.193 (t, $J = 8$, 1 H, 6.338, A′3), 5.913 (d, $J = 8$, 2 H, 6.396/7.171/7.238, B′2), 1.279 (s, 9 H), 1.184 (s, 18 H); spectra are also obtained at 250, 240, 230, 210, and 180 K: complex dynamical processes on the NMR time scale could be seen; $\{^1H\}^{13}C$ NMR (125 MHz, THF-d_8): δ (quaternary or $^1H-^{13}C$ COSY cross-peak, assignment) 293 K, 3-fold-symmetric isomer, 148.3 (q), 144.8 (q), 131.4 (q), 127.9 (6.330, C′3), 125.64 (6.639, C), 124.6 (7.113, C′1), 119.2 (7.163, C), 113.9 (6.664, C′2), 87.2, 34.1, 32.3, 2-fold-symmetric isomer, 149.7 (q), 149.5 (q), 148.0 (q), 146.7 (q), 144.4 (q), 134.3 (q), 129.8 (7.381, A), 129.3 (6.193, A′3), 128.2 (7.171, B′1), 127.7 (6.396, B′3), 125.57 (7.129, A′1), 125.5 (6.681, B), 125.0 (7.193, A), 121.1 (7.277, B), 119.7 (7.238, B′2), 114.9 (5.913, B′2), 114.2 (6.338, A′2), 89.6, 34.8, 34.2, 32.2, 32.0.

ESR Spectroscopy and Quenching Studies of Polyradicals. A solution of carbanion, which was prepared as described above, was transferred with 0.2−0.3 mL of THF to an oxidation vessel.[11] On a vacuum line, 0.5n+ equiv of I_2 (n = number of "unpaired" electrons in a polyradical) were added under a stream of argon to the stirred reaction mixture at −95 °C. Typically, after 0.5 h, the reaction mixture turned yellow/green. 2-MeTHF (~5 mL) from purple sodium/benzophenone was vacuum transferred to the frozen reaction mixture in a liquid nitrogen bath. After the reaction mixture was melted at −95 °C, the oxidation vessel was immersed in a −115 °C bath (EtOH/liquid nitrogen) and a small portion (0.1−0.2 mL) of the reaction mixture was poured to the sidearm ESR tube. The tube was flame sealed and stored in liquid nitrogen.

To the remaining reaction mixture, a drop of Na/K alloy was introduced from the upper part of the reaction vessel. After being stirred at −95 °C for several hours, the color of the reaction mixture changed from yellow/green to red. Following an additional 1−3 days of stirring at −78 °C, MeOH or MeOD (0.3 mL) was added. Aqueous workup gave a crude isomeric mixture of the quenching products.

ESR spectra were acquired with a Bruker 200D instrument, equipped with an Oxford Instruments ESR900 liquid helium cryostat or liquid nitrogen insert dewar, as described elsewhere.[11] The intensities used for the *IT* vs *T* and Curie plots were checked for the microwave saturation by using two or three power settings different by at least 10 dB throughout the studied temperature range; temperatures were stepped up and down in each experiment. Signal-to-noise for the selected spectra in the half- and third-field regions was improved by both time constant/scan time settings and digital addition. The modulation amplitude was kept at or below $^1/_5$ of the estimated peak-to-peak width for all spectra. The microwave frequency was 9.47 GHz in all spectral simulations.

Quenching Products 3-D_4 and 3-H_4. Spectral data for the MeOH-quenching product: ^1H NMR (500 MHz, $CDCl_3$): 7.30−6.83 (m, 28 H), 6.61−6.51 (m, 4 H), 5.42−5.32 (4 peaks, 4 H), 1.31−1.30 (36 H). Separation by PTLC (Analtech silica, ether/hexane, 2/98) gave large R_f (2.5 mg) and small R_f (4.0 mg) fractions. Large R_f fraction (at least two isomers): ^1H NMR (500 MHz, $CDCl_3$): 7.30−6.86 (m, 28 H), 6.56−6.51 (m, 4 H), 5.36 (s, 4 H), 1.303−1.301 (2 singlets, 36 H). $\{^1H\}^{13}C$ NMR (125 MHz, $CDCl_3$): 148.91, 148.85, 144.4, 144.3, 144.2, 140.6, 140.2, 130.23, 130.17, 129.9, 129.2, 129.1, 127.8, 127.7, 127.3, 125.1, 125.0, 56.2, 34.4, 31.4. FABMS (ONPOE), cluster: *m/z* (peak height) at $M^+/(M + H)^+$, 886.5 (1.5), 887.5 (6.5), 888.5 (10), 889.5 (9.5), 890.5 (5), 891.5 (1.5). Small R_f fraction (one isomer): ^1H NMR (500 MHz, EM = −1.1, GB = +0.5, $CDCl_3$): 7.274 (d, $J = 8$, 2 H), 7.265 (d, $J = 8$, 6 H), 7.096 (t, $J = 8$, 2 H), 7.089 (t, $J = 8$, 2 H), 7.020 (d, $J = 8$, 2 H), 6.993 (d, $J = 8$, 6 H), 6.943 (bd, $J = 8$, 2 H), 6.890 (bd, $J = 8$, 2 H), 6.874 (bd, $J = 8$, 2 H), 6.861 (bd, $J = 8$, 2 H), 6.600 (t, $J = 1.5$, 2 H), 6.541 (t, $J = 1.5$, 2 H), 5.38−5.32 (three singlets at 5.36, 5.34, 5.33; 1/2/1, 4 H), 1.31−1.30 (three singlets at 1.308, 1.305, 1.300; 1/1/2, 36 H). $\{^1H\}^{13}C$ NMR (125 MHz, $CDCl_3$): 148.9, 144.4, 144.3, 144.2, 140.7, 140.3, 130.3, 130.2, 129.2, 129.1, 129.0, 127.7, 127.3, 127.2, 127.1, 125.1, 125.0, 56.4, 56.3, 56.2, 34.4, 31.4. FABMS (ONPOE), cluster: *m/z* (peak height) at $M^+/(M + H)^+$, 886.5 (2), 887.5 (6.5), 888.5 (10), 889.5 (9.5), 890.5 (5), 891.5 (1.5).

Spectral data for the MeOD-quenching product: ^1H NMR ($CDCl_3$): 7.30−6.83 (m, 28 H), 6.61−6.51 (m, 4 H), 5.42−5.32 (4 peaks, 0.2 H), 1.31−1.30 (36 H). FABMS (ONPOE), cluster: *m/z* (peak height) at $M^+/(M + H)^+$, 890.6 (7), 891.6 (7.5), 892.6 (10), 893.6 (9.5), 894.6 (5), 895.6 (1.5).

Quenching Products 4-$(H)_3$ and 4-$(D)_3$. The MeOH-quenching product: ^1H NMR ($CDCl_3$): 7.40−6.65 (m, 24 H), 5.40−5.30 (three singlets at 5.38, 5.35, 5.31; 1/2/2; 3 H), 1.35−1.30 (three singlets at 1.33, 1.32, 1.30; 2/2/1; 27 H). Separation by PTLC (silica, hexane/ether, 98/2) gave two isomers: the less polar (*trans* isomer), ^1H NMR ($CDCl_3$, 500 MHz): 7.32 (d, $J = 8$, 4 H), 7.30 (d, $J = 8$, 2 H), 7.15 (d, $J = 8$, 6 H), 7.13−7.01 (m, 4 H), 6.95 (bt, $J = 2$, 2 H), 6.92 (bt, $J = 2$, 1 H), 6.89 (bd, $J = 8$, 2 H), 6.69 (bd, $J = 8$, 2 H), 5.38 (s, 1 H), 5.35 (s, 2 H), 1.32 (s, 18 H), 1.30 (s, 9 H). $\{^1H\}^{13}C$ NMR (125 MHz, $CDCl_3$): 149.2, 145.4, 145.1, 144.7, 139.9, 139.6, 132.1, 129.01, 128.98, 128.1, 127.7, 127.1, 126.6, 125.33, 125.28, 56.5, 34.43, 34.40, 31.4.

FABMS (ONPOE), cluster: *m/z* (peak height) at $M^+/(M + H)^+$, 664.4 (1), 665.4 (7), 666.4 (10), 667.4 (9), 668.4 (4); the more polar (*cis* isomer), ^1H NMR ($CDCl_3$, 500 MHz): 7.34 (d, $J = 8$, 6 H), 7.18 (d, $J = 8$, 6 H), 7.06 (t, $J = 8$, 3 H), 6.87–6.85 (m, 9 H), 5.30 (s, 3 H), 1.33 (s, 27 H). $\{^1H\}^{13}C$ NMR (125 MHz, $CDCl_3$): 149.2, 145.4, 139.5, 132.6, 129.1, 127.7, 126.9, 125.3, 56.5, 34.4, 31.4. FABMS (ONPOE), cluster: *m/z* (peak height) at $M^+/(M + H)^+$, 664.4 (1), 665.4 (6.5), 666.4 (10), 667.4 (9), 668.4 (3.5). The MeOD-quenching product: ^1H NMR ($CDCl_3$): 7.40–6.65 (m, 24 H), 5.40–5.30 (three singlets, <0.2 H), 1.35–1.30 (three singlets at 1.33, 1.32, 1.30; 2/2/1; 27 H). FABMS (ONPOE), cluster: *m/z* (peak height) at $M^+/(M + 1)^+$, 666.4 (1), 667.4 (7.5), 668.4 (7), 669.4 (10), 670.4 (9), 671.4 (4).

Quenching Product 4-H-$(D)_2$. ^1H NMR ($CDCl_3$, 500 MHz): 7.40–6.65 (m, 24 H), 5.40–5.30 (three singlets at 5.38, 5.35, 5.31; 1/1/0.2; 1 H), 1.35–1.30 (three singlets at 1.33, 1.32, 1.30; 0.3/2/1; 27 H). FABMS (ONPOE), cluster: *m/z* (peak height) at $M^+/(M + 1)^+$, 665.4 (<1), 666.4 (4.5), 667.4 (6.5), 668.4 (10), 669.4 (9.5), 670.4 (4), 671.4 (1).

SQUID Magnetometry of Polyradicals. The samples for magnetometry were prepared as described previously,[11] with one exception; i.e., in the case of a dilute sample, additional THF (1–5 mL) was added with a gas-tight Hamilton syringe to the polyradical in THF (0.6–0.8 mL) at low temperature, prior to the transfer to the ESR tube. For dilute samples, two or three 64-point scans of 6-cm length were averaged at each $M(T,H)$ data point at $T \leq 35$ K and $H \leq 5.5$ T, using a Quantum Design MPMS instrument. The M vs H and M vs T data were obtained at $T = 2$, 5, 10 K (and/or 3 K) and $H = 0.5$ or 1.0 T, respectively.

Fitting Procedure for Dilute Samples. (1) The MT vs T plot in the $T = 2$–35 K range is adjusted for residual uncompensated diamagnetism (if any is present); its flatness at high T (beyond saturation) is verified with ESR spectroscopy (IT vs T) for selected polyradicals. (2) The above correction for diamagnetism was applied to M vs H data, accounting for its H dependence. (3) The corrected M vs H data were fit to a Brillouin function as M vs H/T with two variable parameters, S and M_{sat}, at each T separately. If both parameters showed similar values at different temperatures, the M vs H/T fit was judged as satisfactory. If the lower values of S were obtained at the lower T, the mean-field parameter, $\theta < 0$, was used to correct for the antiferromagnetic interactions; i.e., the values θ were adjusted until the fits to M vs $H/(T - \theta)$ with S and M_{sat} were satisfactory. (4) Using M_{sat} from the fit at $T = 2$ K above, the value of S was adjusted until satisfactory fit to MT vs T was obtained. The values of S, which were obtained in points (3) and (4), were within <5%, typically, <2%.

The reliability of the fit, M vs H/T or M vs $H/(T - \theta)$, is measured by parameter dependence between S and M_{sat}, which is defined as follows: *dependence = 1 − [(variance of the parameter, other parameter constant)/(variance of the parameter, other parameters changing)]*. Values close to 1 indicate an overparametrized fit. For the same range of H, the fits were most reliable for the largest values of S and the lowest T.

Acknowledgment. We gratefully acknowledge the National Science Foundation, Chemistry Division for the support of this research (CHE-9203918) and The Camille and Henry Dreyfus Teacher–Scholar Award Program (1991–1996). Mass spectral determinations were performed by the Midwest Center for Mass Spectrometry with partial support by the National Science Foundation, Biology Division (DIR-9017262). We thank Professor Sy-Hwang Liou for access to a SQUID magnetometer and Dr. Andrej Safronov for computer simulations of the ESR spectra.

Supplementary Material Available: Experimental section for synthesis of octaradical $\mathbf{1}^{8\bullet}$ and pentaradical $\mathbf{2}^{5\bullet}$, which were described in the preliminary communication (9 pages). This material is contained in many libraries on microfiche, immediately follows this article in the microfilm version of the journal, and can be ordered from the ACS; see any current masthead page for ordering information.

JA942753P